Characterization of a murine renal distal convoluted tubule cell line for the study of transcellular calcium transport

Robin J. W. Diepens, Els den Dekker, Marcelle Bens, A. Freek Weidema, Alain Vandewalle, René J. M. Bindels and Joost G. J. Hoenderop

Am J Physiol Renal Physiol 286:F483-F489, 2004. First published 18 November 2003;
doi:10.1152/ajprenal.00231.2003

Am J Physiol Renal Physiol 286: F483–F489, 2004.
First published November 18, 2003; 10.1152/ajprenal.00231.2003.

Characterization of a murine renal distal convoluted tubule cell line for the study of transcellular calcium transport

Robin J. W. Diepens,[1] Els den Dekker,[1] Marcelle Bens,[2] A. Freek Weidema,[1] Alain Vandewalle,[2] René J. M. Bindels,[1] and Joost G. J. Hoenderop[1]

[1]*Department of Physiology, Nijmegen Center for Molecular Life Sciences, University Medical Center Nijmegen, NL-6500 HB Nijmegen, The Netherlands; and* [2]*Institut National de la Santé et de la Recherche Médicale, U 478, Faculté de Médecine Xavier Bichat, 75870 Paris Cedex 18, France*

Submitted 24 June 2003; accepted in final form 11 November 2003

Diepens, Robin J. W., Els den Dekker, Marcelle Bens, A. Freek Weidema, Alain Vandewalle, René J. M. Bindels, and Joost G. J. Hoenderop. Characterization of a murine renal distal convoluted tubule cell line for the study of transcellular calcium transport. *Am J Physiol Renal Physiol* 286: F483–F489, 2004. First published November 18, 2003; 10.1152/ajprenal.00231.2003.—To unravel the molecular regulation of renal transcellular Ca^{2+} transport, a murine distal convoluted tubule (mpkDCT) cell line derived from distal convoluted tubules (DCT) microdissected from a SV-PK/Tag transgenic mouse was characterized. This cell line originated from DCT only, as mRNA encoding for the DCT marker thiazide-sensitive Na^+/Cl^- cotransporter was expressed, whereas mRNA encoding for the connecting tubule and collecting duct marker aquaporin-2 was not detected, as determined by reverse-transcriptase PCR. mpkDCT cells expressed mRNA encoding the Ca^{2+} channels TRPV5 and TRPV6 and other key players necessary for transcellular Ca^{2+} transport, i.e., calbindin-D_{9k}, calbindin-D_{28k}, plasma membrane Ca^{2+}-ATPase isoform 1b, and Na^+/Ca^{2+} exchanger 1. Primary cultures of DCT cells exhibited net transcellular Ca^{2+} transport of 0.4 ± 0.1 nmol·h^{-1}·cm^{-2}, whereas net transcellular Ca^{2+} transport across mpkDCT cells was significantly higher at 2.4 ± 0.4 nmol·h^{-1}·cm^{-2}. Transcellular Ca^{2+} transport across mpkDCT cells was completely inhibited by ruthenium red, an inhibitor of TRPV5 and TRPV6, but not by the voltage-operated Ca^{2+} channel inhibitors felodipine and verapamil. With the use of patch-clamp analysis, the IC_{50} of ruthenium red on Na^+ currents was between the values measured for TRPV5- and TRPV6-expressing HEK 293 cells, suggesting that TRPV5 and/or TRPV6 is possibly active in mpkDCT cells. Forskolin in combination with IBMX, 1,25-dihydroxyvitamin D_3, and 1-deamino-8-D-arginine vasopressin increased transcellular Ca^{2+} transport, whereas PMA and parathyroid hormone had no significant effect. In conclusion, the murine mpkDCT cell line provides a unique cell model in which to study the molecular regulation of transcellular Ca^{2+} transport in the kidney in vitro.

TRPV5; TRPV6; vitamin D_3; kidney; calcium reabsorption

Ca^{2+} HOMEOSTASIS is regulated by Ca^{2+} absorption by the intestine, storage in and release from bones, and by reabsorption and excretion by the kidney. In the kidney, 98% of the filtered Ca^{2+} is reabsorbed, whereas only 2% is excreted in the urine (10). The majority of Ca^{2+} reabsorption occurs by paracellular transport in the proximal part of the nephron. In the distal part of the nephron, mainly in the distal convoluted tubule (DCT) and the connecting tubule (CNT), transcellular Ca^{2+} transport is the main route for Ca^{2+} reabsorption, which accounts for only 10–20% of total Ca^{2+} reabsorption by the kidney. However, this represents a key portion for regulated Ca^{2+} reabsorption, because transcellular Ca^{2+} transport in the distal part of the nephron is tightly controlled by calciotropic hormones (3, 33, 34).

Transcellular Ca^{2+} transport can be divided into three processes: Ca^{2+} entry at the apical side, intracellular translocation, and extrusion at the basolateral side. The recently discovered highly selective Ca^{2+} channels TRPV5 and TRPV6 (also known as ECaC1 and ECaC2, respectively) at the apical side of cells are the main Ca^{2+} entry sites (15, 21, 23, 25). Calbindins-D_{9k} and -D_{28k} are intracellular Ca^{2+}-binding proteins that are thought to participate in shuttling Ca^{2+} from the apical to the basolateral membrane (5, 12, 19, 36), where the Na^+/Ca^{2+} exchanger (NCX1) and the plasma membrane Ca^{2+}-ATPase 1b (PMCA1b) account for Ca^{2+} extrusion (24, 33, 40).

The calciotropic hormone 1,25-dihydroxyvitamin D_3 [$1,25(OH)_2D_3$] tightly regulates transcellular Ca^{2+} transport. It is active at all three processes necessary for transcellular Ca^{2+} transport. $1,25(OH)_2D_3$ stimulates mRNA expression of the Ca^{2+} entry channels TRPV5 and TRPV6 (22), calbindins-D_{9k} and -D_{28k} (13, 22), and PMCA1b (18). Currently, the molecular regulation of transcellular Ca^{2+} transport in DCTs remains elusive, because in vivo transcellular Ca^{2+} transport assays are difficult to perform. We describe here for the first time a cell system, which approaches the endogenous physiological state of DCTs in mice, in which the regulation of transcellular Ca^{2+} transport can be studied.

MATERIALS AND METHODS

Cell culture. Studies were performed on mpkDCT cells (38) microdissected from the kidney of an SV-PK/Tag transgenic mouse carrying the SV-40 large T and small t antigens under control of the SV-40 enhancer placed in front of the −1,000-bp fragment of the rat L-L′-PK gene regulatory region in the 5′-flanking region (30). The murine distal convoluted tubule (mpkDCT) cells have been established using the same protocol described for the establishment of the differentiated cortical collecting duct (CD) principal mpkCCD$_{cl4}$ cells (1, 11). mpkDCT cells were cultured in a defined medium with minor modifications: DMEM/Ham's F-12 medium (1:1 vol/vol; Invitrogen, Breda, The Netherlands) supplemented with 2% (vol/vol) heat-inactivated FCS, 5 μg/ml insulin (Sigma, St. Louis, MO), 5 nM dexamethasone (Sigma), 90 nM sodium selenate (Sigma), 5 μg/ml transferrin (Sigma), 1 nM triiodothyronine (Sigma), 10 ng/ml EGF (Sigma), 0.2% D-glucose (Sigma), 20 mM HEPES (GIBCO, Breda, The Netherlands), 4.5 mM glutamine (GIBCO), and 45 μg/ml gentamicin at pH 7.4, equilibrated with 5% CO_2-95% air at 37°C. For

Address for reprint requests and other correspondence: J. Hoenderop, 160 Physiology, Univ. Medical Center Nijmegen, P.O. Box 9101, NL-6500 HB Nijmegen, The Netherlands (E-mail: J.Hoenderop@ncmls.kun.nl).

The costs of publication of this article were defrayed in part by the payment of page charges. The article must therefore be hereby marked "*advertisement*" in accordance with 18 U.S.C. Section 1734 solely to indicate this fact.

routine passage, cells were grown in T25 plastic culture flasks and passaged every 3–4 days when 80% confluent. For $^{45}Ca^{2+}$ transport studies, and RNA isolation, $\sim 5 \cdot 10^4$ cells were seeded on collagen-coated permeable membrane filter inserts (6.5-mm internal diameter, 0.4-μm pore size; Costar) and cultured for 6 days; medium was changed on *day 3*. Just before every study, the transepithelial electrical resistance (TEER) was determined as a measure for confluence of the monolayer, using a volt-ohm meter (Millipore, Etten-Leur, The Netherlands). As controls, experiments were performed on confluent monolayers of primary cultured DCT cells. Isolated late DCT cells were microdissected from the kidneys of wild-type C57BL6 9- to 12-wk-old female mice using the same protocol used for primary cultures of microdissected cortical CDs (2). Briefly, mice were killed by cervical dislocation. Kidneys were rapidly removed under sterile conditions and incubated in the same medium described above and supplemented with collagenase A (0.1% wt/vol, Roche Diagnostic, Mannheim, Germany) for 45 min at 37°C. Distal tubules were then microdissected out under sterile condition as described before (2). Isolated DCTs (8–10 fragments, 0.2- to 0.5-mm long) were seeded on collagen-coated permeable membrane filter inserts and grown in the same defined medium described above. After 5 days, the medium was changed every 2 days. Experiments were carried out 2 wk after seeding, and just before every study, the TEER was determined as a measure for confluence of the monolayer, using a volt-ohm meter. All experiments were performed in accordance with the guidelines of the French and Dutch Agricultural Offices and in compliance with legislation governing animal studies.

$^{45}Ca^{2+}$ transport assay. Transport studies were conducted as described previously, with minor modifications (4, 13). Briefly, confluent monolayers were incubated in Krebs-Henseleit buffer containing 110 mM NaCl, 5 mM KCl, 1.2 mM $MgCl_2$, 10 mM sodium acetate, 20 mM HEPES, 2 mM NaH_2PO_4, 4 mM L-lactate, 10 mM D-glucose, 1 mM L-alanine adjusted to pH 7.4 using 1 M Tris, supplemented with 1 mM $CaCl_2$, 10 μM felodipine, 10 μM verapamil, 1 mM $BaCl_2$, 2 μCi $^{45}CaCl_2$/ml, and with the drug of choice: 10 μM forskolin (Sigma) and 100 μM IBMX (Sigma), 100 nM PMA (Sigma), 100 nM $1,25(OH)_2D_3$ (Solvay, Weesp, The Netherlands), ruthenium red (RR; 100 nM, 1, 10, and 100 μM; Fluka, St. Louis, MO), 100 nM bovine parathyroid hormone (bPTH) (1–34) (Sigma), or 10 nM 1-deamino-8-D-arginine vasopressin (dDAVP). All drugs were added to the apical side as well as to the basolateral side of the monolayer, except for RR, which was added to the apical side only. Cells were incubated at 37°C for 60 min. Subsequently, aliquots of 10% of the total volume were taken from the contralateral side, and radioactivity was measured using a liquid scintillation counter. $^{45}Ca^{2+}$ transport from the basolateral to the apical side was subtracted from the $^{45}Ca^{2+}$ transport from the apical-to-basolateral side to determine the net transport.

RT-PCR. Total RNA was isolated using the TRIzol isolation method according to manufacturer's protocol (GIBCO). RNA was treated for 1 h at 37°C with RNAse-free DNAse to remove any contaminating genomic DNA. DNAse was heat inactivated at 65°C using a 10-min incubation. Subsequently, 2 μg of total RNA were reverse transcribed in a 30-μl reaction volume containing 6 μl 5× first-strand buffer (Invitrogen), 3 μl 0.1 M DTT, 2 μl 10 mM dNTP, 0.5 μg random hexamer primers (Promega, Leiden, The Netherlands), 20 U RNAse inhibitor (Promega), and 200 U Moloney murine leukemia virus reverse transcriptase (Invitrogen) at 37°C for 90 min, followed by incubation for 5 min at 90°C. PCR amplification was performed in a 50-μl volume using 3 μl RT-sample, 1 μl *Taq* polymerase, 1× Cetus buffer [10 mM Tris·HCl, 50 mM KCl, 0.01% (vol/vol) gelatin, and 2.5 mM $MgCl_2$], 1 mM dNTPs, and 0.2 μM of each primer. For RT-PCR, the following protocol was used: 1 min at 95°C; followed by 40 cycles for 1 min at 95°C, 1 min at the correct annealing temperature (see Table 1) and 1 min at 72°C; followed by 10 min at 72°C. An actin RT^- sample was used as a negative control and was run for 60 cycles at an annealing temperature of 50°C. Primers targeting the genes of interest are listed in Table 1.

Electrophysiology. Electrophysiological methods for measuring Na^+ and Ca^{2+} currents related to TRPV5 and TRPV6 channel activity have been described previously in detail (39). Patch-clamp experiments were performed in the whole cell configuration, using an EPC-9 patch-clamp amplifier (HEKA Elektronik, Lambrecht, Germany). Patch pipettes had DC resistances of 2–4 MΩ when filled with intracellular solution. A ramp protocol, consisting of linear voltage ramps from +100 to −100 mV within 450 ms, was applied every 2 s from a holding potential of +20 mV. Current densities, expressed per unit membrane capacitance, were calculated from the current at −80 mV during ramp protocols. The internal (pipette) solution contained 20 mM CsCl, 100 mM Cs aspartate, 1 mM $MgCl_2$, 10 mM BAPTA, 4 mM Na_2ATP, and 10 mM HEPES/CsOH, pH 7.2. The external solution contained 1 mM $CaCl_2$, 150 mM NaCl, 6 mM CsCl, 1 mM $MgCl_2$, 10 mM HEPES/NaOH (pH 7.4), 10 mM glucose, and different concentrations of RR (100 nM-100 μM). Divalent-free solutions did not contain added divalent cations, while trace amounts of divalent cations were removed with 100 μM EDTA. All experiments were performed at room temperature (20–24°C).

Statistics. In all experiments, data are expressed as means ± SE. Statistical significance was determined by Student's *t*-test. Differences in means with $P < 0.05$ were considered statistically significant.

RESULTS

mpkDCT cell line possesses specific properties of DCTs. mpkDCT cells were derived from isolated DCTs, microdissected from the kidney of an adult transgenic mouse (SV-PK/

Table 1. *Sequences of primers for RT-PCR*

Gene	Forward Primer	Reverse Primer	Product	Annealing Temp	No. of Cycles
TRPV5	5′-CGTTGGTTCTTACGGGTTGAAC-3′	5′-GTTTGGAGAACCACAGAGCCTCTA-3′	168	50°C	40
TRPV6	5′-ATCCGCCGCTATGCACA-3′	5′-AGTTTTTCTCCTGAATCTTTTTCCAA-3′	80	50°C	40
CaBP-D_{9k}	5′-CCTGCAGAAATGAAGAGCATTTT-3′	5′-CTCCATCGCCATTCTTATCCA-3′	175	50°C	40
CaBP-D_{28k}	5′-AACTGACAGAGATGGCCAGGTTA-3′	5′-TGAACTCTTTCCCACACATTTTGAT-3′	87	50°C	60
PMCA 1b	5′-CGCCATCTTCTGCACCATT-3′	5′-CAGCCATTGCTCTATTGAAAGTTC-3′	109	50°C	40
NCX1	5′-TCCCTACAAAACTATTGAAGGCACA-3′	5′-TTTCTCATACTCCTCGTCATCGATT-3′	142	50°C	60
CaSR	5′-CTTTCCTATCCATTTTGGAGTAGCA-3′	5′-GCAAAGATCATGGCTTGTAACCA-3′	120	50°C	40
NCC	5′-GTGGGTGTGGCCATGCAC-3′	5′-GTCCAGAAAATGGCCATGAG-3′	461	60°C	60
AQP2	5′-CCAGTGGGCCAGCTCCCCAC-3′	5′-AACCGATGACGGCGCCCACC-3′	551	60°C	60
PTHr	5′-GCACACAGCAGCCAACATAA-3′	5′-CGCAGCATAAACGACAGGAA-3′	531	54°C	40
β-Actin	5′-ACGATTTCCCTCTCAGCTGTG-3′	5′-GTATGCCTCTGGTCGTACCAC-3′	201	50°C	40

PCR primers were purchased from Biolegio. Product size is in base pairs. CaBP-D_{9k} and $-D_{28k}$, calbindin $-D_{9k}$ and $-D_{28k}$; PMCA 1b, plasma-membrane Ca^{2+}-ATPase 1b; NCX1, Na^+/Ca^{2+} exchanger; CaSR, calcium-sensing receptor; NCC, Na^+-Cl^- cotransporter; AQP2, aquaporin-2; PTHr, parathyroid hormone receptor.

TAG) (11, 32). To demonstrate the origin of nature of this microdissected DCT cell line, the expression of typical markers for DCT, CNT, and CD was determined using RT-PCR analysis. As shown in Fig. 1*A*, mpkDCT cells expressed NCC, which is a marker for DCT, but did not express aquaporin-2 (AQP2), known to be expressed in CNT and CD. To determine whether the mpkDCT cell line is suitable for the study of transcellular Ca^{2+} transport, the mRNA expression of key players involved in this process was investigated using RT-PCR. As shown in Fig. 1*B*, all the constituents of the transcellular Ca^{2+} transport process, including TRPV5, TRPV6, calbindin-D_{9k}, calbindin-D_{28k}, PMCA1b, NCX1, and CaSR, were expressed in the mpkDCT cell line.

Transcellular Ca^{2+} transport by cultured murine DCT cells. Primary cultures of isolated late DCT cells microdissected from the kidneys of wild-type C57BL6 mice and grown on permeable filters were used to assess the Ca^{2+} transport capacities of the murine DCT and compared with that of the established cultured mpkDCT cells. Mean TEER across a monolayer of primary cultures of DCT cells, grown for 2 wk on collagen-coated permeable filter supports, was determined at 2,389 ± 148 $\Omega \cdot cm^2$ (n = 14), whereas the mean TEER across a monolayer of mpkDCT cells, cultured for 6 days on collagen-coated permeable filter supports, was determined at 1,790 ± 88 $\Omega \cdot cm^2$ (n = 23). Net Ca^{2+} transport was calculated by subtracting basolateral-to-apical Ca^{2+} transport from apical-to-basolateral Ca^{2+} transport. As shown in Fig. 2, both primary cultures of DCT cells and the mpkDCT cell line

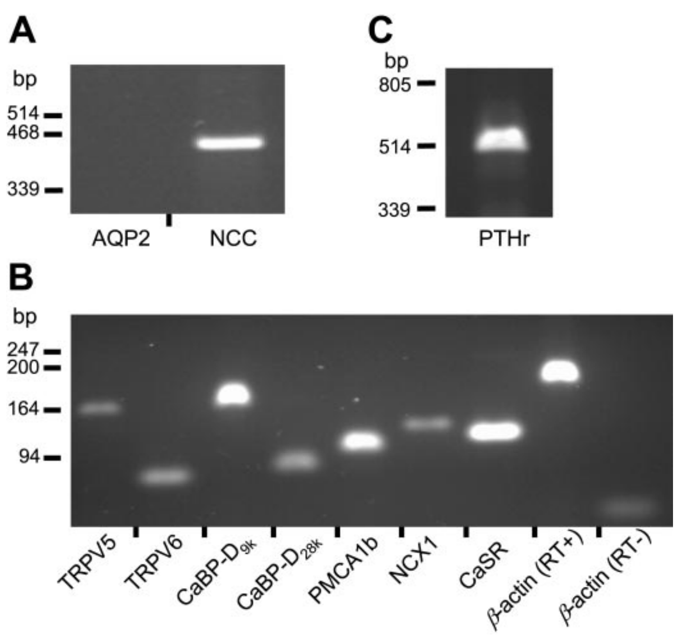

Fig. 1. Characterization of murine distal convoluted tubule (mpkDCT) cells by RT-PCR. mpkDCT cells were grown on permeable membrane filter supports until confluency. *A*: detection of aquaporin-2 (AQP2) mRNA and thiazide-sensitive Na^+-Cl^- cotransporter (NCC) mRNA. *B*: detection of mRNA encoding for TRPV5, TRPV6, calbindin-D_{9k} (CaBP-D_{9k}), calbindin-D_{28k} (CaBP-D_{28k}), plasma membrane Ca^{2+} ATPase 1b (PMCA1b), Na^+/Ca^{2+} exchanger 1 (NCX1), Ca^{2+}-sensing receptor (CaSR). β-Actin was used as a control to demonstrate the integrity of the isolated RNA. As a negative control, a PCR (60 cycles) on β-actin was performed on a RT− sample. *C*: detection of mRNA encoding the parathyroid hormone receptor (PTHr) in mpkDCT cells.

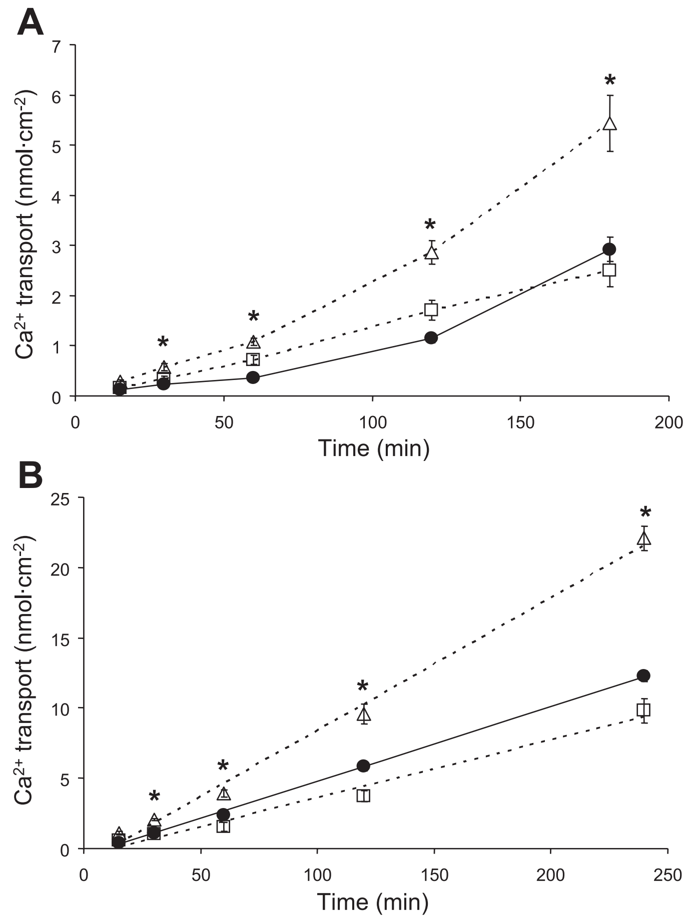

Fig. 2. $^{45}Ca^{2+}$ transport across cultured distal convoluted tubule (DCT) cell monolayers. Transcellular Ca^{2+} transport was measured at various time points between 15 and 180 min. Basolateral-to-apical transport was subtracted from apical-to-basolateral transport to determine net Ca^{2+} transport. △, Apical-to-basolateral transport; □, basolateral-to-apical transport; ●, net transport. *A*: $^{45}Ca^{2+}$ transport across primary cultures of DCT cells. *B*: $^{45}Ca^{2+}$ transport across the mpkDCT cell line. Data are presented as means ± SE ($n \geq 6$ per time point). **P* < 0.05; apical-to-basolateral transport significantly different from basolateral-to-apical transport.

exhibited significantly higher apical-to-basolateral transport than basolateral-to-apical transport from 15 min onward. Net Ca^{2+} transport across primary cultures of DCT cells was 0.4 ± 0.1 $nmol \cdot h^{-1} \cdot cm^{-2}$ (Fig. 2*A*), whereas net Ca^{2+} transport across the mpkDCT cell line was significantly higher (2.4 ± 0.2 $nmol \cdot h^{-1} \cdot cm^{-2}$; Fig. 2*B*). The calculated net Ca^{2+} transport for the mpkDCT cell line was linear for up to 4 h after addition of $^{45}Ca^{2+}$. In subsequent experiments, net Ca^{2+} transport was calculated using the 60-min time point.

Ca^{2+} transport across mpkDCT cells is RR sensitive. To study RR-sensitive transcellular Ca^{2+} transport independent of voltage-operated Ca^{2+} channels, verapamil (10 μM) and felodipine (10 μM) were added apically as well as basolaterally to the transport buffer in all experiments performed to block voltage-operated Ca^{2+} channels, and $BaCl_2$ (1 mM) was added to prevent changes in membrane potential. With the use of different concentrations of RR, the IC_{50} of RR for the blockage of transcellular Ca^{2+} transport was determined. For mpkDCT cells, the IC_{50} of RR on the Na^+ current was 8.8 ± 0.3 μM (Fig. 3). In this study, the IC_{50} of RR on the Na^+ current of

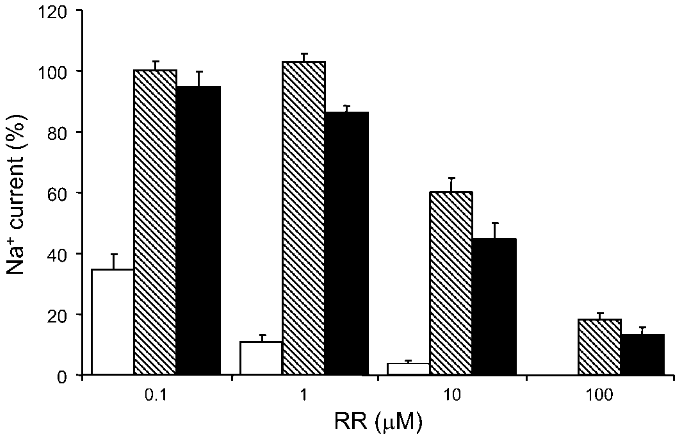

Fig. 3. Electrophysiological analysis of mpkDCT cells. Ruthenium red (RR) inhibition of Na^+ currents in HEK 293 cells overexpressing TRPV5 (open bars), HEK 293 cells overexpressing TRPV6 (hatched bars), and mpkDCT cells (filled bars) is shown. Data are presented as means ± SE ($n \geq 10$ cells).

TRPV5- and TRPV6-expressing human embryonic kidney 293 cells (HEK 293 cells) was determined at <0.1 and 17.5 ± 0.6 μM, respectively, as determined by patch-clamp analysis. Net $^{45}Ca^{2+}$ transport measured in the mpkDCT cells was inhibited by RR with an IC_{50} of 2.2 ± 0.7 μM (Fig. 4), a value that is on the same order of magnitude as the value determined by patch-clamp analysis.

cAMP and 1,25(OH)$_2$D$_3$ increased transcellular Ca^{2+} transport in mpkDCT cells. It has been shown that an increase of intracellular cAMP triggers stimulation of Ca^{2+} reabsorption in the kidney. Other studies showed that Ca^{2+} reabsorption is stimulated on activation of the PKC pathway (14, 20). Therefore, the effect of a rise in cAMP and stimulation of PKC on transcellular Ca^{2+} transport was studied in the mouse mpkDCT cell line. Forskolin (10 μM) in combination with IBMX (100 μM) increased Ca^{2+} transport by 92 ± 13% compared with nontreated cells (Fig. 5). This rise was completely inhibited by 100 μM RR, indicating that the stimulation induced by the PKA pathway reflected is possibly mediated by TRPV5 and/or TRPV6. On the other hand, the PKC activator

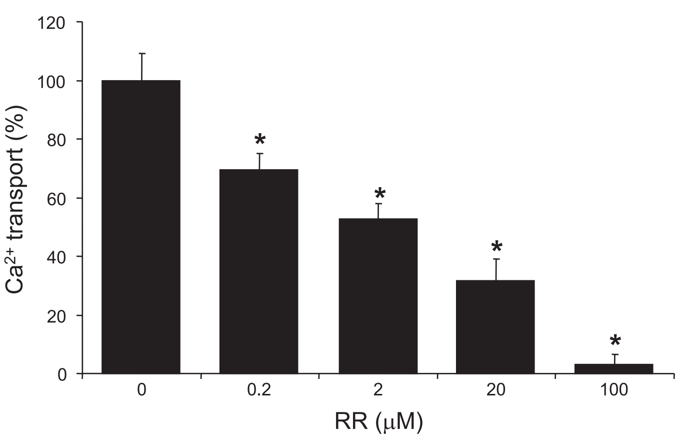

Fig. 4. Inhibition of $^{45}Ca^{2+}$ transport across mpkDCT cells by RR. mpkDCT cell monolayers were incubated with different concentrations of RR (0, 0.2, 2, 20, and 200 μM) in the presence of tracer $^{45}Ca^{2+}$ for 60 min at 37°C. Net $^{45}Ca^{2+}$ transport in nontreated mpkDCT cells was 3.5 ± 0.3 nmol·h^{-1}·cm^{-2} and was set to 100% to which all values are related. Data are presented as means ± SE ($n \geq 6$). $^*P < 0.05$ significantly different from control value.

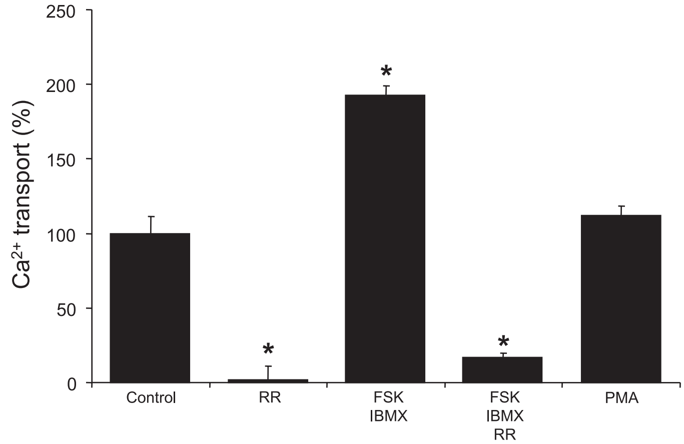

Fig. 5. Effect of PKA and PKC pathway stimulation on Ca^{2+} transport across mpkDCT monolayers. Confluent mpkDCT cell monolayers were incubated with RR (100 μM), forskolin (FSK; 10 μM)/IBMX (100 μM), or PMA (100 nM) in the presence of tracer $^{45}Ca^{2+}$ for 60 min at 37°C. Ca^{2+} transport in nontreated cells was 3.1 ± 0.4 nmol·h^{-1}·cm^{-2} and was set at 100%, to which all values are related. Data are presented as means ± SE (n = 5). $^*P < 0.05$ significantly different from control value.

PMA did not induce a rise in Ca^{2+} transport across confluent monolayers of mpkDCT cells (Fig. 5).

To study the effect of physiologically relevant calciotropic hormones, confluent mpkDCT cells were incubated with either 1,25(OH)$_2$D$_3$ (100 nM), bPTH (1–34) (100 nM), or dDAVP (10 nM) during the Ca^{2+} transport experiment. mpkDCT cells were incubated for 72 h with 1,25(OH)$_2$D$_3$ (100 nM) to determine the long-term effects on Ca^{2+} transport. As shown in Fig. 6*A*, both dDAVP and long-term stimulation with 1,25(OH)$_2$D$_3$ increased Ca^{2+} transport with 119 ± 7 and 70 ± 21%, respectively, compared with nontreated cells. 1,25(OH)$_2$D$_3$- and dDAVP-stimulated Ca^{2+} transport was significantly inhibited by RR (Fig. 6*A*). Because bPTH had no significant effect on transcellular Ca^{2+} transport, PTH derived from rat (Sigma) and bovine (NIBSC, Herts, UK) was also tested. Although PTHr was detected at the mRNA level (Fig. 1*C*), none of the tested PTH batches affected Ca^{2+} transport. Gesek and Friedman (17) showed a significant effect of PTH on $^{45}Ca^{2+}$ influx in a mixture of DCT and cortical thick ascending limb (cTAL) cells, which was abolished by nifedipine. In the absence of felodipine, verapamil, and $BaCl_2$, PTH did not stimulate transcellular Ca^{2+} transport in mpkDCT cells (Fig. 6*B*). Moreover, transcellular Ca^{2+} transport across mpkDCT cells is primarily regulated by RR-sensitive channels and not by dihydropyridine-sensitive channels.

DISCUSSION

The present study demonstrated that the mpkDCT cell line established from transgenic SV-PK/Tag mouse distal tubules is a valuable cell system in which to study transcellular Ca^{2+} transport in the DCT in vitro. This conclusion is based on the following observations: *1*) mpkDCT cells express the key players necessary for transcellular Ca^{2+} transport: the epithelial Ca^{2+} channels TRPV5 and TRPV6, the intracellular Ca^{2+} translocators calbindin-D$_{9k}$ and calbindin-D$_{28k}$, and the basolateral Ca^{2+} extrusion proteins NCX1 and PMCA1b; *2*) mpkDCT cells exhibit a significant net apical-to-basolateral Ca^{2+} transport; *3*) RR completely inhibits net Ca^{2+} transport, sug-

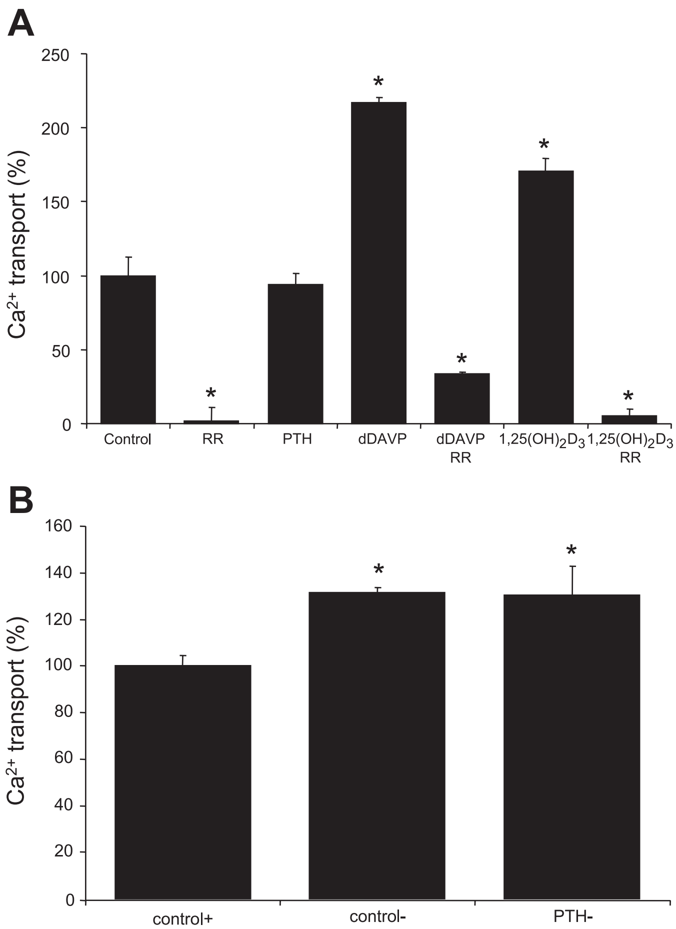

Fig. 6. Effect of 1,25-dihydroxyvitamin D_3 [$1,25(OH)_2D_3$], 1-deamino-8-D-arginine vasopressin (dDAVP), and parathyroid hormone (PTH) on Ca^{2+} transport across mpkDCT monolayers. *A*: confluent mpkDCT cells were incubated with RR (100 μM), $1,25(OH)_2D_3$ (100 nM, 72 h), dDAVP (10 nM), or PTH (100 nM) in the presence of tracer $^{45}Ca^{2+}$ for 60 min at 37°C. Net Ca^{2+} transport in these experiments was 2.7 ± 0.3 nmol·h^{-1}·cm^{-2} and set at 100%, to which all values are related. *B*: confluent mpkDCT cells in the presence (control+) or absence (control−) of verapamil (10 μM), felodipine (10 μM), and $BaCl_2$ (1 mM) were stimulated with PTH (100 nM). Net Ca^{2+} transport across mpkDCT cells treated with verapamil, felodipine, and $BaCl_2$ was 4.6 ± 0.2 nmol·h^{-1}·cm^{-2} and set at 100%, to which all values are related. Data are presented as means ± SE ($n \geq 3$ filters per condition). *$P < 0.05$ significantly different from control value.

gesting a possible role for TRPV5 and/or TRPV6 in transcellular Ca^{2+} transport in mpkDCT cells; *4*) stimulation of the cAMP/PKA pathway by forskolin in combination with IBMX increases net Ca^{2+} transport twofold; and *5*) $1,25(OH)_2D_3$ and dDAVP increase Ca^{2+} transport to the same extent as observed with cAMP/PKA pathway activation.

Confluent mpkDCT cells grown on filters developed high TEER, clearly indicating that the mpkDCT cell line forms tight monolayers. The observed TEER values are in line with observations reported by Peng et al. (32), who first described the mpkDCT cell line and demonstrated that the mpkDCT cells formed confluent monolayers of epithelial cells. Subsequently, Van Huyen et al. (38) clearly demonstrated a polarized monolayer of mpkDCT cells as assessed by staining for Na^+-K^+-ATPase in the basolateral membrane.

The distal part of the nephron consists of cTAL, DCT, CNT, and CD. To determine the origin of the murine mpkDCT cell line derived from late DCTs, AQP2 and NCC expression was determined. The CNT and CD marker AQP2 (9, 16) was not expressed in mpkDCT cells, whereas the DCT marker NCC (6, 28, 29) was present. These results demonstrated that the mpkDCT cell line possesses the expression profile of mouse DCT cells.

Ca^{2+} reabsorption in the distal part of the nephron is stimulated by several hormones including PTH, $1,25(OH)_2D_3$, calcitonin, and vasopressin (26). PTH, calcitonin, and vasopressin bind to surface receptors that activate the trimeric G protein G_s, leading to an increase in the cAMP level and subsequent activation of PKA (8, 37). However, other studies suggested that PKC activation is an important mechanism leading to the observed increase in Ca^{2+} reabsorption in the distal part of the nephron (14, 20). In the study of regulation of Ca^{2+} transport in confluent layers of mpkDCT cells, it was found that stimulation of PKC by PMA had no effect on transcellular Ca^{2+} transport, whereas a rise in cAMP caused by the addition of forskolin/IBMX significantly increased Ca^{2+} transport. Using RR, the increase in transcellular Ca^{2+} transport due to forskolin/IBMX stimulation could be completely inhibited, suggesting that the observed effect is due to RR-sensitive transcellular Ca^{2+} transport, possibly mediated by TRPV5 and/or TRPV6. These findings point to a role of the cAMP/PKA pathway, but not the PKC pathway, in regulating Ca^{2+} transport in DCT cells. This is in line with previous findings of our laboratory (20), that the dose-response curve for the increase in cAMP virtually matched that for transcellular Ca^{2+} transport in CNT and CD. The mechanism by which cAMP activates Ca^{2+} transport remains to be elucidated. It is unlikely that phosphorylation of TRPV5 and/or TRPV6 channels by PKA is involved, as the potential PKA phosphorylation sites are not species conserved. The mpkDCT cell line thus represents a valuable tool for unraveling the mechanism of hormone-mediated stimulation of transcellular Ca^{2+} transport.

$1,25(OH)_2D_3$ stimulated the Ca^{2+} transport by 70% across monolayers of mpkDCT cells grown on permeable filters. Previously, it was shown that $1,25(OH)_2D_3$ increases the mRNA expression level of both Ca^{2+} channels TRPV5 and TRPV6 (22, 27), calbindin-D_{9k} and calbindin-D_{28k} (13, 22), and PMCA1b (18). Together with the increased transport on stimulation by $1,25(OH)_2D_3$, this clearly demonstrated that the effect of $1,25(OH)_2D_3$ is due to transcriptional regulation of Ca^{2+}-transporting proteins, which is consistent with previous results (22).

Transcellular Ca^{2+} transport across mpkDCT cells increased by ~100% on stimulation with dDAVP, whereas PTH had no significant effect on transcellular Ca^{2+} transport, which is in line with previous studies in which PTH does not stimulate adenylate cyclase in the DCT but does affect adenylate cyclase activity in the cTAL, CNT, and CD of the nephron (31). Another study also reported that PTH does not stimulate Ca^{2+} transport in the DCT, whereas 8-(*p*-chlorophenylthio)-adenosine 3′,5′-cyclic monophosphate exhibits a stimulatory effect (35). On the other hand, Chabardes et al. (7) showed a PTH-dependent stimulation of adenylate cyclase activity in the mouse DCT and Peng et al. (32) demonstrated a minor but significant increase in the cAMP content after PTH stimulation in mpkDCT cells, whereas dDAVP increased cellular cAMP levels ~82-fold in these cells. Gesek and Friedman (17) demonstrated a stimulating effect of PTH on $^{45}Ca^{2+}$ influx in a mixture of DCT and cTAL cells, which was abolished by nifedipine. The present study indicates that PTH has no significant effect on transcellular Ca^{2+} transport in mpkDCT cells in the absence of felodipine, verapamil, and $BaCl_2$, suggesting that the described dihydropyridine- and PTH-sensitive Ca^{2+} channels (17) are not present in the mpkDCT cells.

The aim of the present study was to develop a cell line that can be of value in elucidating the molecular mechanism controlling transcellular Ca^{2+} transport in the DCT. We postulate a possible role for TRPV5 and/or TRPV6 in mpkDCT cells, which is based on the following observations: *1*) mpkDCT cells express TRPV5 and TRPV6 on mRNA level; *2*) mpkDCT cells exhibit functional transcellular Ca^{2+} transport, which is regulated by $1,25(OH)_2D_3$; *3*) mpkDCT cells show an IC_{50} for RR, which is in line with the affinities for TRPV5/6; and *4*) mpkDCT cells display strong inward rectifying currents (data not shown), which could be blocked by RR. Because specific blockers for TRPV5 and TRPV6 are not yet available, it is at present difficult to demonstrate conclusively that these Ca^{2+} channels are solely responsible for the transcellular Ca^{2+} transport process observed in mpkDCT cells.

In conclusion, the findings of the present study clearly demonstrate that the transimmortalized mpkDCT cell line exhibits transcellular Ca^{2+} transport and has maintained many characteristics of native DCT cells, including expression of TRPV5 and TRPV6. This cell line thus provides a valuable tool for investigating short-term (regulatory) and long-term (transcriptional) control of renal transcellular Ca^{2+} reabsorption.

GRANTS

This study was financially supported by grants from the Dutch Organization of Scientific Research (Zon-Mw 902.18.298, Zon-Mw 016.006.001).

REFERENCES

1. **Bens M, Vallet V, Cluzeaud F, Pascual-Letallec L, Kahn A, Rafestin-Oblin ME, Rossier BC, and Vandewalle A.** Corticosteroid-dependent sodium transport in a novel immortalized mouse collecting duct principal cell line. *J Am Soc Nephrol* 10: 923–934, 1999.
2. **Bens M, Van Huyen JP, Cluzeaud F, Teulon J, and Vandewalle A.** CFTR disruption impairs cAMP-dependent Cl^- secretion in primary cultures of mouse cortical collecting ducts. *Am J Physiol Renal Physiol* 281: F434–F442, 2001.
3. **Bindels RJ.** Calcium handling by the mammalian kidney. *J Exp Biol* 184: 89–104, 1993.
4. **Bindels RJ, Hartog A, Timmermans J, and Van Os CH.** Active Ca^{2+} transport in primary cultures of rabbit kidney CCD: stimulation by 1,25-dihydroxyvitamin D_3 and PTH. *Am J Physiol Renal Fluid Electrolyte Physiol* 261: F799–F807, 1991.
5. **Bindels RJ, Hartog A, Timmermans JA, and van Os CH.** Immunocytochemical localization of calbindin-D_{28k}, calbindin-D_{9k} and parvalbumin in rat kidney. *Contrib Nephrol* 91: 7–13, 1991.
6. **Campean V, Kricke J, Ellison D, Luft FC, and Bachmann S.** Localization of thiazide-sensitive Na^+-Cl^- cotransport and associated gene products in mouse DCT. *Am J Physiol Renal Physiol* 281: F1028–F1035, 2001.
7. **Chabardes D, Imbert-Teboul M, Gagnan-Brunette M, and Morel F.** Different hormonal target sites along the mouse and rabbit nephrons. *Curr Probl Clin Biochem* 8: 447–454, 1977.
8. **Chabre O, Conklin BR, Lin HY, Lodish HF, Wilson E, Ives HE, Catanzariti L, Hemmings BA, and Bourne HR.** A recombinant calcitonin receptor independently stimulates 3′,5′-cyclic adenosine monophosphate and Ca^{2+}/inositol phosphate signaling pathways. *Mol Endocrinol* 6: 551–556, 1992.
9. **Coleman RA, Wu DC, Liu J, and Wade JB.** Expression of aquaporins in the renal connecting tubule. *Am J Physiol Renal Physiol* 279: F874–F883, 2000.
10. **Costanzo LS and Windhager EE.** Renal regulation of calcium balance. In: *The Kidney: Physiology and Pathophysiology*, edited by Seldin DW and Giebisch G. New York: Raven, 1992, p. 2375–2393.
11. **Duong Van Huyen J, Bens M, and Vandewalle A.** Differential effects of aldosterone and vasopressin on chloride fluxes in transimmortalized mouse cortical collecting duct cells. *J Membr Biol* 164: 79–90, 1998.
12. **Feher JJ, Fullmer CS, and Wasserman RH.** Role of facilitated diffusion of calcium by calbindin in intestinal calcium absorption. *Am J Physiol Cell Physiol* 262: C517–C526, 1992.
13. **Fleet JC and Wood RJ.** Identification of calbindin-D_{9k} mRNA and its regulation by 1,25-dihydroxyvitamin D_3 in Caco-2 cells. *Arch Biochem Biophys* 308: 171–174, 1994.
14. **Friedman PA and Gesek FA.** Cellular calcium transport in renal epithelia: measurement, mechanisms, and regulation. *Physiol Rev* 75: 429–471, 1995.
15. **Fullmer CS.** Intestinal calcium absorption: calcium entry. *J Nutr* 122: 644–650, 1992.
16. **Fushimi K, Uchida S, Hara Y, Hirata Y, Marumo F, and Sasaki S.** Cloning and expression of apical membrane water channel of rat kidney collecting tubule. *Nature* 361: 549–552, 1993.
17. **Gesek FA and Friedman PA.** On the mechanism of parathyroid hormone stimulation of calcium uptake by mouse distal convoluted tubule cells. *J Clin Invest* 90: 749–758, 1992.
18. **Glendenning P, Ratajczak T, Dick IM, and Prince RL.** Calcitriol upregulates expression and activity of the 1b isoform of the plasma membrane calcium pump in immortalized distal kidney tubular cells. *Arch Biochem Biophys* 380: 126–132, 2000.
19. **Gross M and Kumar R.** Physiology and biochemistry of vitamin D-dependent calcium binding proteins. *Am J Physiol Renal Fluid Electrolyte Physiol* 259: F195–F209, 1990.
20. **Hoenderop JG, De Pont JJ, Bindels RJ, and Willems PH.** Hormone-stimulated Ca^{2+} reabsorption in rabbit kidney cortical collecting system is cAMP-independent and involves a phorbol ester- insensitive PKC isotype. *Kidney Int* 55: 225–233, 1999.
21. **Hoenderop JG, Muller D, Suzuki M, van Os CH, and Bindels RJ.** Epithelial calcium channel: gate-keeper of active calcium reabsorption. *Curr Opin Nephrol Hypertens* 9: 335–340, 2000.
22. **Hoenderop JG, Muller D, Van Der Kemp AW, Hartog A, Suzuki M, Ishibashi K, Imai M, Sweep F, Willems PH, Van Os CH, and Bindels RJ.** Calcitriol controls the epithelial calcium channel in kidney. *J Am Soc Nephrol* 12: 1342–1349, 2001.
23. **Hoenderop JG, Nilius B, and Bindels RJ.** ECaC: the gatekeeper of transepithelial Ca^{2+} transport. *Biochim Biophys Acta* 1600: 6–11, 2002.
24. **Hoenderop JG, Nilius B, and Bindels RJ.** Molecular mechanisms of active Ca^{2+} reabsorption in the distal nephron. *Annu Rev Physiol* 64: 529–549, 2002.
25. **Hoenderop JG, van der Kemp AW, Hartog A, van de Graaf SF, van Os CH, Willems PH, and Bindels RJ.** Molecular identification of the apical Ca^{2+} channel in 1,25-dihydroxyvitamin D_3-responsive epithelia. *J Biol Chem* 274: 8375–8378, 1999.
26. **Hoenderop JG, Willems PH, and Bindels RJ.** Toward a comprehensive molecular model of active calcium reabsorption. *Am J Physiol Renal Physiol* 278: F352–F360, 2000.
27. **Li H and Christakos S.** Differential regulation by 1,25-dihydroxyvitamin D_3 of calbindin-D_{9k} and calbindin-D_{28k} gene expression in mouse kidney. *Endocrinology* 128: 2844–2852, 1991.
28. **Loffing J and Kaissling B.** Sodium and calcium transport pathways along the mammalian distal nephron: from rabbit to human. *Am J Physiol Renal Physiol* 284: F628–F643, 2003.
29. **Loffing J, Loffing-Cueni D, Valderrabano V, Klausli L, Hebert SC, Rossier BC, Hoenderop JG, Bindels RJ, and Kaissling B.** Distribution of transcellular calcium and sodium transport pathways along mouse distal nephron. *Am J Physiol Renal Physiol* 281: F1021–F1027, 2001.
30. **Miquerol L, Cluzeaud F, Porteu A, Alexandre Y, Vandewalle A, and Kahn A.** Tissue specificity of L-pyruvate kinase transgenes results from the combinatorial effect of proximal promoter and distal activator regions. *Gene Expr* 5: 315–330, 1996.
31. **Morel F, Chabardes D, and Imbert M.** Functional segmentation of the rabbit distal tubule by microdetermination of hormone-dependent adenylate cyclase activity. *Kidney Int* 9: 264–277, 1976.
32. **Peng KC, Cluzeaud F, Bens M, Van Huyen JP, Wioland MA, Lacave R, and Vandewalle A.** Tissue and cell distribution of the multidrug

resistance-associated protein (MRP) in mouse intestine and kidney. *J Histochem Cytochem* 47: 757–768, 1999.
33. **Reilly RF and Ellison DH.** Mammalian distal tubule: physiology, pathophysiology, and molecular anatomy. *Physiol Rev* 80: 277–313, 2000.
34. **Rouse D and Suki WN.** Renal control of extracellular calcium. *Kidney Int* 38: 700–708, 1990.
35. **Shimizu T, Yoshitomi K, Nakamura M, and Imai M.** Effects of PTH, calcitonin, and cAMP on calcium transport in rabbit distal nephron segments. *Am J Physiol Renal Fluid Electrolyte Physiol* 259: F408–F414, 1990.
36. **Stein WD.** Facilitated diffusion of calcium across the rat intestinal epithelial cell. *J Nutr* 122: 651–656, 1992.
37. **Van Baal J, Raber G, de Slegte J, Pieters R, Bindels RJ, and Willems PH.** Vasopressin-stimulated Ca^{2+} reabsorption in rabbit cortical collecting system: effects on cAMP and cytosolic Ca^{2+}. *Pflügers Arch* 433: 109–115, 1996.
38. **Van Huyen JP, Bens M, Teulon J, and Vandewalle A.** Vasopressin-stimulated chloride transport in transimmortalized mouse cell lines derived from the distal convoluted tubule and cortical and inner medullary collecting ducts. *Nephrol Dial Transplant* 16: 238–245, 2001.
39. **Vennekens R, Hoenderop JG, Prenen J, Stuiver M, Willems PH, Droogmans G, Nilius B, and Bindels RJ.** Permeation and gating properties of the novel epithelial Ca^{2+} channel. *J Biol Chem* 275: 3963–3969, 2000.
40. **Wasserman RH, Chandler JS, Meyer SA, Smith CA, Brindak ME, Fullmer CS, Penniston JT, and Kumar R.** Intestinal calcium transport and calcium extrusion processes at the basolateral membrane. *J Nutr* 122: 662–671, 1992.